arXiv:hep-ex/0202023v1 11 Feb 2002

# RESULTS FROM HIGH ENERGY ACCELERATORS

G. GIACOMELLI and B. POLI

*Dept of Physics, Univ. of Bologna and INFN,*
*V.le C. Berti Pichat 6/2, Bologna, I-40127, Italy*
E-mail: giacomelli@bo.infn.it , barbara.poli@bo.infn.it

Lectures at the $6^{th}$ School on Non-Accelerator Astroparticle Physics,
Trieste, Italy, 9-20 July 2001.

**Abstract**

We review some of the recent experimental results obtained at high-energy colliders with emphasis on LEP and SLC results.

## 1 Introduction

High energy colliders allow to study two particle collisions at the highest energies, since the c.m. energy $\sqrt{s}$ grows linearly with the beam energy $E_b$: $\sqrt{s} = 2E_b$. In particular $e^+e^-$ collisions offer the possibility of studying in the simplest way the fundamental particles and their basic interactions[1]. The highest energy collider is the Tevatron at Fermilab with c.m. energies up to 2 TeV. The highest energy $e^+e^-$ collider was LEP2 at CERN; it was closed in november 2000. LEP, the SLC linear collider at SLAC and the Tevatron tested the Standard Model (SM) of electroweak and strong interactions to unprecedented precisions [1]-[3].

Besides energy, the second important parameter of a collider is its luminosity $\mathcal{L}$, which is defined as that number which multiplied by a cross-section $\sigma$ gives the collision rate $N$ : $N = \mathcal{L}\sigma$. The highest energy $e^+e^-$ colliders have or had luminosities in the range $10^{31} < \mathcal{L} < 10^{32}\ cm^{-2}s^{-1}$, which yield collision rates of $\sim 1$ event/s at $\sqrt{s} = m_Z$ and $\sim$0.01 event/s at LEP2 ($130 < \sqrt{s} < 208$ GeV). Recent $e^+e^-$ b-factories have much larger luminosities.

In these notes we shall first summarize the legacy of LEP to high energy physics and shall then discuss some results from other high energy accelerators.

Fig. 1 shows the cross–section for $e^+e^- \rightarrow$ hadrons vs $\sqrt{s}$. Precise measurements of the $Z^0$ mass, width, and decay properties yield precision tests of the electroweak (EW) theory. In the SM the $Z^0$ decay width is related to the number of fermion pairs into which it can decay. The more ways in which it can decay, the faster it decays and the wider the $Z^0$ peak becomes. Measurements of the $Z^0$ width constrain the number of generations (3 neutrino families), and deviations from an integer value may hint at new physics. Radiative corrections modify the Breit–Wigner shape of

the $Z^0$ resonance. The analyses of radiative corrections yielded below threshold a precise value for the top–quark mass, in excellent agreement with the directly measured value [2].

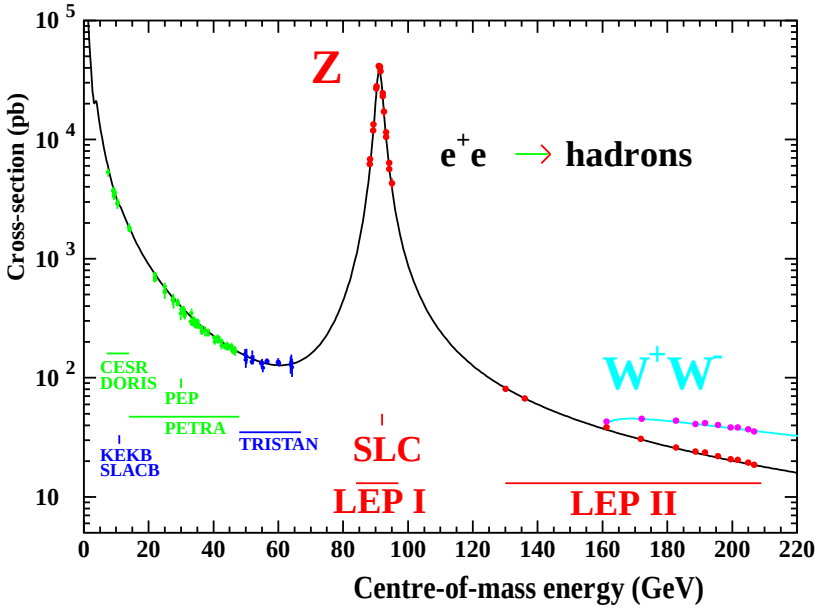


Figure 1: Energy dependence of $\sigma(e^+e^- \rightarrow \text{hadrons})$.

Since the $Z^0$ decays predominantly into quark–antiquark pairs, it yields a clean data sample with which to test quantum chromodynamics (QCD), the theory of the strong interaction. The $q\bar{q}$ pair is never observed directly, but it gives rise to two opposite jets of hadrons by a process called fragmentation (hadronization). Before fragmentation takes place, one of the quarks may radiate a gluon by a process similar to bremsstrahlung. In this case, three jets of hadrons are produced. The ratio of the number of three–jet events to the number of two–jet events is one way of measuring $\alpha_s$, the strong coupling constant, which is a fundamental parameter of QCD.

In addition to the quarks, the leptons and the vector bosons, the SM requires at least one scalar Higgs particle (the $H^0_{SM}$ ), which is needed for the hypothesized mechanism for the generation of masses. The coupling of the Higgs particle is predicted by the theory, but not its mass. The precision measurements at the $Z^0$ yield indirect information on the $H^0_{SM}$ mass. A direct limit and a hint of a Higgs boson were obtained at LEP2.

The higher energies and luminosities at LEP2 allowed to study the triple boson vertex in $e^+e^- \rightarrow Z^0 \rightarrow W^+W^-$, measure with precision the mass and the width of $W^{\pm}$, perform searches for new particles.

Experiments at the HERA $e^+p$ collider provided information on the proton structure at the

lowest x-values and largest Q-values; they studied the photon structure, heavy flavour production, leading proton physics, hadronic final states and performed many searches for new particles.

Eperiments at the Fermilab $p\bar{p}$ collider found the top quark above threshold, provided precise measurements of $m_t$ and $m_W$, studied quark and gluon collisions at the highest energies, yielding large $p_t$ events, studied minimum bias, low $p_t$ physics and performed many new particle searches.

Recent experiments at fixed target accelerators gave information on direct CP violation in the $K^0\bar{K}^0$ system [4], while experiments at b-factories gave the first indications of CP violation in the $B^0\bar{B}^0$ system [5].

Among the very many results obtained in fixed target experiments at accelerators, we mention very briefly: the study of Deep Inelastic Scattering (DIS) with longitudinally polarized $\mu^-$ and $e^-$ on protons in sophisticated experiments at CERN and SLAC; they found that only 30% of the proton spin is carried by the valence quarks; it would seem that the main fraction of the proton spin is carried by gluons [6].

# 2 Experimental

Most of the recent high energy physics data come from high energy colliders, where several large, $4\pi$, general purpose detectors may operate simultaneously. Each of them is made of many subdetectors, whose combined role is to measure the energy, direction, charge, and type of the particles produced. Apart from neutrinos, no particle should be able to escape a detector without leaving some sign of its passage. Each subdetector has a cylindrical structure, with a "barrel" and two "end-caps". Tracking is performed by a central detector, whilst electron and photon energy measurements are carried out by a high–resolution electromagnetic calorimeter; the magnet iron yoke is instrumented as a hadron calorimeter; it is followed by a muon detector. At $e^+e^-$ colliders, a forward detector completes the e.m. coverage by tagging small–angle electrons and photons, and is used as a precision luminosity monitor.

In order to select and measure the cross–section for a specific channel, one needs: (i) a trigger, (ii) the required events ($N_i$), (iii) the computation of the global efficiency ($\epsilon_i$), and (iv) a luminosity determination ($\int \mathcal{L}\, dt$): $\sigma_i = N_i/(\epsilon_i \int \mathcal{L}\, dt)$ . Recent improvements concern the vertex detectors, in view of studying short lived particles and for direct searches for the $H^0_{SM}$, for example in $e^+e^- \to Z^0 \to Z^0 + H^0_{SM} \to Z^0 + b\bar{b}$.

# 3 $e^+e^-$ collisions. The LEP legacy

## 3.1 Electroweak physics

At energies around the $Z^0$ peak the basic processes are

$$\mathrm{e^+e^-} \to Z^0, \gamma \to f\bar{f}\ , \qquad f\bar{f} = q\bar{q}, \ell\bar{\ell}, \tag{1}$$

The $\ell\bar{\ell}$ pairs may be charged ($\mathrm{e^+e^-}$, $\mu^+\mu^-$, $\tau^+\tau^-$) or neutral ($\nu_\mathrm{e}\bar{\nu}_\mathrm{e}$, $\nu_\mu\bar{\nu}_\mu$, $\nu_\tau\bar{\nu}_\tau$) leptons. The $q\bar{q}$ pairs are $\mathrm{u\bar{u}}$, $\mathrm{d\bar{d}}$, $\mathrm{s\bar{s}}$, $\mathrm{c\bar{c}}$, and $\mathrm{b\bar{b}}$ (the $\mathrm{t\bar{t}}$ has a higher energy threshold). Each $q$ or $\bar{q}$ hadronizes in a

jet of hadrons. Thus the $q\bar{q}$ pairs are characterized by two opposite jets of hadrons. The $q$ (or the $\bar{q}$) may radiate a gluon, which yields a third jet.

The behaviour of any cross–section around the $Z^0$ peak is typical of a resonant state with $J = 1$, described by a relativistic Breit–Wigner formula, plus an electromagnetic term and an interference term:

$$\begin{array}{rcccccc} \sigma(e^+e^- \to f\bar{f}) = & \frac{4}{3}\pi\frac{\alpha(m_Z^2)}{s} & + & I\frac{s-m_Z^2}{s} & + & \frac{12\pi}{m_Z^2}\Gamma_{e^+e^-}\Gamma_{f\bar{f}}\frac{s}{(s-m_Z^2)^2+\frac{s^2}{m_Z^2}\Gamma_Z^2} \\ & \text{electrom.} & & \text{interf.} & & \text{resonant} & \\ & \text{term} & & \text{term} & & \text{term} & \end{array} \tag{2}$$

This formula has to be convoluted with initial state radiation. Around the $Z^0$, the first two terms of Eq. 2 are small corrections to the main term, which is the $Z^0$ Breit–Wigner. $\Gamma_{f\bar{f}}$ is the partial width for the decay of the $Z^0$ into a fermion–antifermion pair, $Z^0 \to f\bar{f}$. The total width $\Gamma_Z$ is given by

$$\Gamma_Z = \Gamma_\mathrm{h} + \Gamma_\mathrm{e} + \Gamma_\mu + \Gamma_\tau + N_\nu\Gamma_\nu = \Gamma_\mathrm{vis} + \Gamma_\mathrm{inv} \ , \tag{3}$$

where $\Gamma_\mathrm{h}$ is the hadronic width and $\Gamma_\mathrm{e}, \Gamma_\mu, \Gamma_\tau, \Gamma_\nu$ are the leptonic widths; it is costumary to use $R_e = \Gamma_\mathrm{h}/\Gamma_\mathrm{e}$, $R_\mu = \Gamma_\mathrm{h}/\Gamma_\mu$ and $R_\tau = \Gamma_\mathrm{h}/\Gamma_\tau$. In the Standard Model

$$\left\{ \begin{array}{rcl} \Gamma_\mathrm{h} & = & \Gamma_\mathrm{u} + \Gamma_\mathrm{d} + \Gamma_\mathrm{s} + \Gamma_\mathrm{c} + \Gamma_\mathrm{b} = 1742 \text{ MeV} \\ \Gamma_\mathrm{u} & = & \Gamma_\mathrm{c} = 296 \text{ MeV} \quad , \quad \Gamma_\mathrm{d} = \Gamma_\mathrm{s} = \Gamma_\mathrm{b} = 374 \text{ MeV} \\ \Gamma_\mathrm{e} & = & \Gamma_\mu = \Gamma_\tau = 84.0 \text{ MeV} \\ \Gamma_\nu & = & 167.3 \text{ MeV} \quad , \quad N_\nu = 3 \quad , \quad \Gamma_\mathrm{inv} = 501.6 \text{ MeV} \\ \Gamma_\mathrm{Z} & = & \Gamma_\mathrm{h} + 3\Gamma_\ell + 3\Gamma_\nu = 2495 \text{ MeV} \ . \end{array} \right. \tag{4}$$

In the electroweak theory each partial width $\Gamma_f$ may be expressed in terms of vector ($g_v$) and axial–vector ($g_a$) coupling constants

$$g_a = I_{3\mathrm{f}} \quad , \quad g_v = I_{3\mathrm{f}} - 2Q_\mathrm{f}\sin^2\theta_\mathrm{w} \ , \tag{5}$$

where $I_{3\mathrm{f}}$ is the third component of the weak isospin, $Q_\mathrm{f}$ the electric charge of the fermion and $\theta_\mathrm{w}$ the weak mixing angle:

$$\Gamma_f = N_\mathrm{c}\frac{G_\mu\ m_Z^3}{6\pi\sqrt{2}}(g_v^2 + g_a^2)(1 + \delta_f) \tag{6}$$

$N_\mathrm{c}$ is the number of colours ($N_\mathrm{c} = 1$ for leptons, $N_\mathrm{c} = 3$ for quarks), $\delta_f$ accounts for QED+EW corrections. Angular distributions of the produced $f\bar{f}$ exhibit asymmetries; at $m_Z$ they are written as

$$A_\mathrm{FB}^{0,f} = \frac{3}{4}A_\mathrm{e}A_f \quad , \quad A_f = \frac{2g_vg_a}{g_v^2 + g_a^2} \ . \tag{7}$$

Fig. 2 shows the energy dependence of $\sigma(e^+e^- \to \text{hadrons}(\gamma))$ and of $\sigma(e^+e^- \to l^+l^-(\gamma))$, without removing, and removing, radiative events; the SM predictions (lines) are in agreement with the data (points) [7].

At energies $\sqrt{s} > 100$ GeV the probability of radiating a photon by the initial $e^+$ or $e^-$ is high; thus the effective collision energy $\sqrt{s'} < \sqrt{s}$; the distribution in $\sqrt{s'}$ indicates clearly a peak at the $Z^0$ resonance.

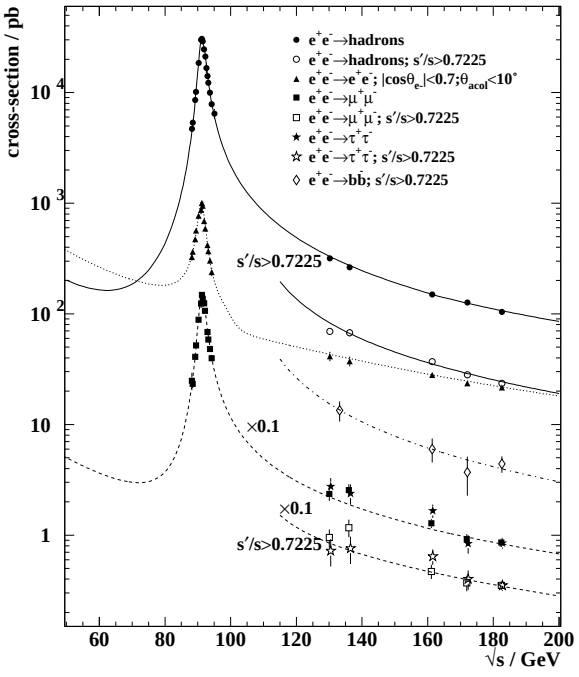


Figure 2: $e^+e^-$ cross sections vs c.m. energy.

## 3.2 Radiative corrections

Radiative corrections for the processes $e^+e^- \to f\bar{f}$ include QED, EW and QCD corrections, which may be summarized by the Feynman diagrams of Fig. 3.

**QED radiative corrections** : (i) photon emission from the initial state $e^+$, $e^-$ modifies the effective c.m. energy and distorts the Breit–Wigner shape of the $Z^0$ resonance. (ii) QED radiative corrections + EW and QCD corrections lead to the running of the electromagnetic coupling costant

$$\alpha_{\rm QED}(s) = \frac{\alpha_{\rm QED}(m_Z^2)}{1 - \Delta\alpha_{\rm l}(s) - \Delta\alpha_{\rm h}^{(5)} - \Delta\alpha_{\rm top}(s)} \tag{8}$$

where $\Delta\alpha_{\rm l}(s)$ and $\Delta\alpha_{\rm top}(s)$ are well known; $\Delta\alpha_{\rm h}^{(5)}$ arises from the contribution of light quarks to the photon vacuum polarization; this correction may be computed using the new $e^+e^-$ data obtained by the BES experiment in China for energies below 12 GeV [8]. The new determination $\Delta\alpha_{\rm h}^{((5)}(m_Z^2) = 0.02761 \pm 0.00036$ has a smaller error than previous determinations [9]. On the other hand the same new BES data plus more theoretical input in the low energy region lead to

$\Delta\alpha_{\rm h}^{(5)}(m_Z^2) = 0.02738 \pm 0.00020$ [10].

**EW radiative corrections** : they lead to corrections to the coupling costants of the $Z^0$ to

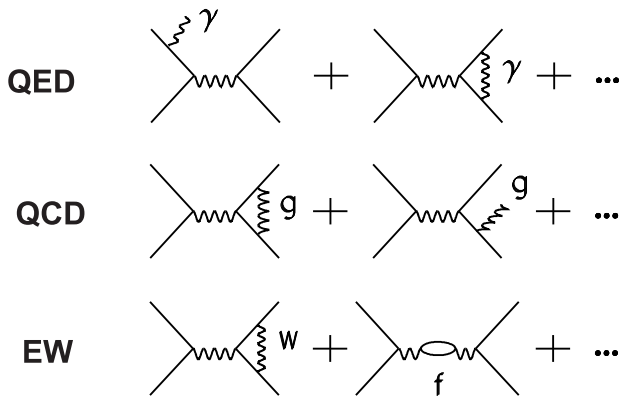


Figure 3: Radiative correction diagrams.

fermions. These corrections may be absorbed in the definitions (i) of the electroweak mixing angle

$$\sin^2\theta_{\rm W} = 1 - \frac{m_{\rm W}^2}{m_{\rm Z}^2} \quad \Rightarrow \quad \sin^2\theta_{\rm eff}^{\rm lept} = (1+\Delta{\rm K})\sin^2\theta_{\rm W} \tag{9}$$

(ii) of the $\rho$ parameter:

$$\rho = \frac{m_{\rm W}^2}{m_{\rm Z}^2\cos^2\theta_{\rm W}} = 1 \quad \Rightarrow \quad \tilde{\rho} = 1 + \Delta\rho \tag{10}$$

(iii) of $m_{\rm W}$:

$$m_{\rm W}^2 = \frac{\pi\alpha}{\sqrt{2}\sin^2\theta_{\rm W}G_{\rm f}}(1+\Delta r), \qquad \Delta r = \Delta\alpha_{\rm QED} + \Delta r_{\rm W} \tag{11}$$

The corrections are therefore summarized in $\Delta K$, $\Delta\rho$, $\Delta r_{\rm W}$, which depend quadratically on $m_{\rm top}$ and logarithmically on $m_{\rm H^0}$.

**QCD radiative corrections** : they are difficult to compute; different techniques must be used for each particular problem considered. For example, perturbation theory of a fixed order is adequate for the total cross section. Neglecting strong corrections and quark masses, the total hadronic width of the $Z^0$ boson can be written as $\Gamma_{\rm h} = \Sigma_q\ \Gamma_q$ where $\Gamma_q$ is given in Eq. 6. The strong radiative corrections, to order $\alpha_s^3$, modify $\Gamma_{\rm h}$, which can now be expressed as

$$\Gamma'_{\rm h} = \Gamma_{\rm h}\left[1 + c_1\frac{\alpha_s}{\pi} + c_2(\frac{\alpha_s}{\pi})^2 + c_3(\frac{\alpha_s}{\pi})^3\right], \tag{12}$$

where $c_1$, $c_2$ and $c_3$ have been calculated.

Fixed order perturbation theory is not adequate for QCD calculations in the back–to–back region where large logarithmic factors can arise, destroying the convergence of the perturbative expansion. Resummation at all orders of perturbation theory is necessary and was done for different variables.

### 3.3 Precision measurements

At each energy around the $Z^0$ peak, measurements of the cross–sections have been carried out for $e^+e^- \to Z^0 \to$ hadrons, $e^+e^-$, $\mu^+\mu^-$, $\tau^+\tau^-$, the forward–backward lepton asymmetries $A_{\rm FB}^{\rm e}$, $A_{\rm FB}^{\mu}$, $A_{\rm FB}^{\tau}$, the $\tau$ polarization asymmetry $P_\tau$, the $\rm b\bar{b}$ and $\rm c\bar{c}$ partial widths and forward–backward asymmetries, and the $q\bar{q}$ charge asymmetries. As time goes on more parameters are added. The latest one is $m_W$, whose determination improves every year (see Table 1). These measurements plus informations from $\nu N$ and $\overline{p}p$ collisions allow to make precise tests of the SM and constrain the Higgs boson mass. In summary the measured quantities are:

From LEP1 + SLC

Mass and width of the $Z^0$ $\qquad m_Z,\ \Gamma_Z = \Gamma_{\rm h} + \Gamma_{\rm e} + \Gamma_\mu + \Gamma_\tau + N_\nu \Gamma_\nu$

$$\begin{cases} \text{Hadronic cross section at } \sqrt{\rm s} = {\rm m_{Z^0}} & \sigma_0^{\rm h} \\ \text{Ratios at } \sqrt{\rm s} = {\rm m_{Z^0}} & {\rm R_l^0} = \frac{\Gamma_{\rm h}}{\Gamma_{\rm l}}\ ({\rm l = e}, \mu, \tau),\ {\rm R_b^0},\ {\rm R_c^0} \\ \text{Asymmetries at } \sqrt{\rm s} = {\rm m_{Z^0}} & {\rm A_{FB}^{0,l}} = (\frac{\rm N_F - N_B}{\rm N_F + N_B})^{0,\rm l},\ {\rm A_{FB}^{0,b\bar{b}}},\ {\rm A_{FB}^{0,c\bar{c}}} \\ \text{The } \tau \text{ polarization parameter} & {\rm P}_\tau \end{cases}$$

From SLC

The left-right asymmetry $\ {\rm A}_{LR}^0$ and the leptonic LR-FB asymmetry $\ {\rm A}_{FB}^{LR}$ measured with polarized beams

From LEP2 + p$\bar{p}$ $\qquad {\rm m}_W$

From p$\bar{p}$ $\qquad {\rm m}_t$

The LEP, SLC and $p\bar{p}$ experiments give to the LEP working group (WG) their measured values; the WG makes averages which are used in the fits.

**Early fits**: They yielded precise tests of

– lepton universality: $\quad R_e = R_\mu = R_\tau, \quad A_e = A_\mu = A_\tau,$

– number of neutrino families: $\quad N_\nu = 2.9841 \pm 0.0083.$

**Latest fits** [2],[3]: **(i)** Fit without the measured values of $\rm m_W$, $\rm m_t$. This fit "below threshold" yields values of $\rm m_t$, $\rm m_W$, $\rm m_{H^0_{SM}}$:

$$\rm m_t = 169.0\ ^{+11.5}_{-8.9}\ GeV, \quad m_W = 80.363 \pm 0.032\ GeV, \quad m_{H^0_{SM}} = 81\ ^{+109}_{-40}\ GeV,$$

which can be compared with the measured values of $m_t$, $m_W$:

$$m_t = 174.3 \pm 5.1 \text{ GeV}, \quad m_W = 80.448 \pm 0.034 \text{ GeV}$$

The agreement of the direct and indirect determinations of $m_t$, $m_W$ shows the consistency of the SM.

**(ii)** Global fit [2],[3]: including all data (also $m_t$, $m_W$) and new $\Delta\alpha^{(5)}_h$ corrections. The fit has $\chi^2/DoF = 22.9/15$ and yields the following values of $m_t$, $m_W$, $m_{H^0_{SM}}$:

$$m_t = 175.8 \pm 4.3 \text{ GeV}, \quad m_W = 80.398 \pm 0.019 \text{ GeV}, \quad m_{H^0_{SM}} = 88 \ {}^{+53}_{-35} \text{ GeV}$$

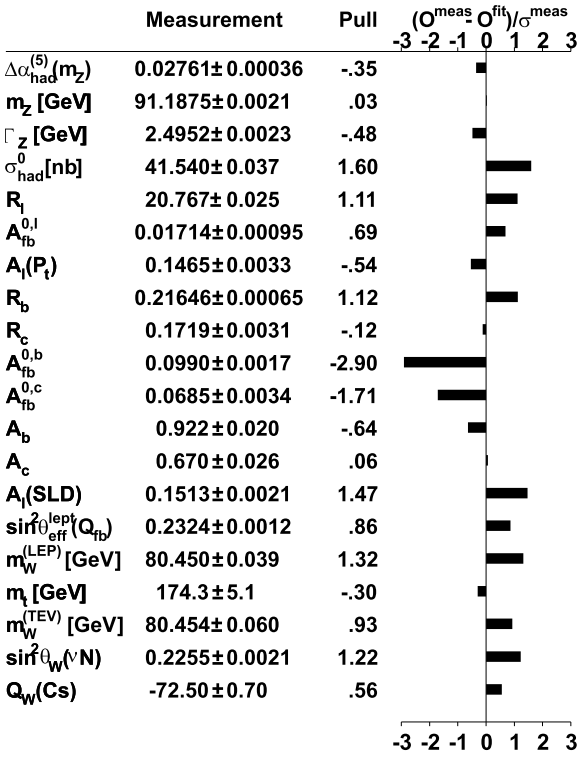


Figure 4: Precise measurements of the electroweak parameters obtained from the global fit, and the pull parametrs $= \left[O^{meas} - O^{fit}\right]/\sigma^{meas}$ [3].

Fig. 4 gives the values of the quantities obtained from the global fit and the pull parameters. The fit is not very good; this comes mainly from $A^{0,b}_{FB}$: it could be a statistical fluctuation, an

error in the measurement of $A_{FB}^{0,b}$ or a hint of physics beyond the SM. Checks are been made on all the measurements of $A_{FB}^{0,b}$. We point out that the present precision on $\sin^2\theta_W$, $m_W$ and $m_Z$ are almost two orders of magnitude better than what anticipated in 1984.

Fig. 5 shows a comparison of several determinations of $\sin^2\theta_{eff}^{lept}$ from measurements of different asymmetries; it also shows the prediction of the SM as a function of the Higgs boson mass.

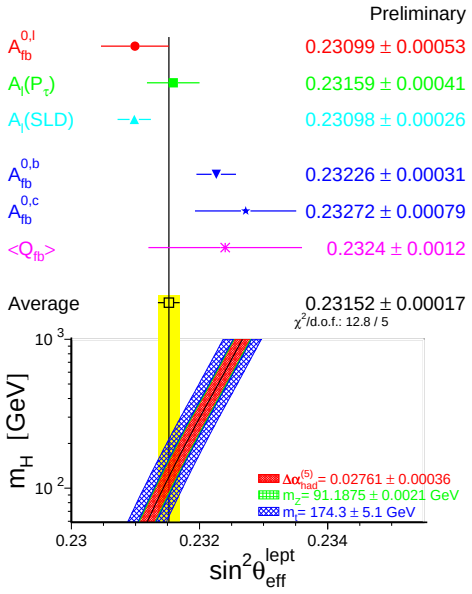


Figure 5: Determinations of $\sin^2\theta_{eff}^{lept}$ from different asymmetries. Also shown is the SM prediction as function of $m_{H_{SM}^0}$.

### 3.4 The SM Higgs boson

Fig. 6 shows the $\chi^2$ of the global fit as a function of $m_{H_{SM}^0}$ for two values of $\Delta\alpha_h^{(5)}$. The fit indicates that at the 95% CL the $H_{SM}^0$ mass should be lower than 196 GeV [2],[3].

The direct search for the SM Higgs boson is performed via the reaction $e^+e^- \rightarrow Z^0 \rightarrow Z^0 + H_{SM}^0$, considering all possible decays for the $Z^0$ and $H_{SM}^0$ ($Z^0 \rightarrow f\bar{f}$, $H_{SM}^0 \rightarrow f'\bar{f}'$) [11]. The $H_{SM}^0$ prefers to decay into the heaviest particles; thus the channel $H_{SM}^0 \rightarrow b\bar{b}$ has the highest branching ratio. For this reason all microvertex detectors were upgraded for the LEP2 phase in order to cover the largest angular range for $b\bar{b}$ with the highest efficiency. The search suffers from SM processes which simulate Higgs boson candidates. Complex procedures based on likelihood

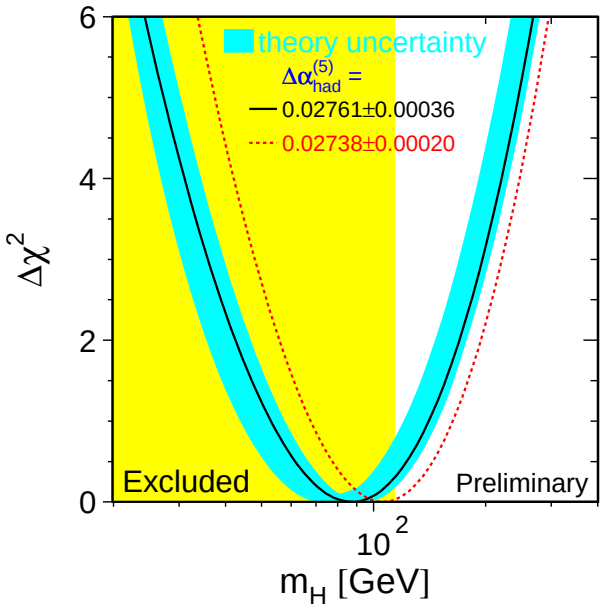


Figure 6: $\Delta\chi^2 = \chi^2 - \chi^2_{min}$ vs $m_{H^0_{SM}}$. The solid line is the result of the fit using all data, the band rapresents an estimate of the theoretical error due to missing higher order corrections. The vertical band shows the 95% CL exclusion limit on $m_H$ from the direct search. The dashed curve is the result obtained using a different evaluation of $\Delta\alpha^{(5)}_{\rm h}(m^2_Z)$, see text.

methods have been deviced to cope with this background. The present situation for the $H^0_{SM}$ search at LEP2 may summarized saying that there is a signal for a preferred mass of 115.6 GeV; the probability that the background may simulate the signal is 3.4%. Thus the indication (evidence) for a SM Higgs is at the level of about 2.5 standard devations. From the same combination of data, a the 95% CL lower bound is obtained: $m_{H^0_{SM}} > 114.1$ GeV [12],[13].

### 3.5 Multihadronic events

Multihadron production in $e^+e^-$ annihilations proceeds via four distinct phases.
i) In the first phase the initial $e^+e^-$ pair annihilates into a virtual $Z^0/\gamma$, which yields a $q\bar{q}$ pair: this phase is described by the EW perturbative theory, and occurs at distances of the order of $10^{-17}$ cm. Before annihilation, a $\gamma$ may be emitted by the initial $e^+$ or $e^-$, thus reducing the effective c.m. energy.
ii) In the second phase the $q$ (or the $\bar{q}$) may radiate a gluon, which subsequently radiates a second gluon (yielding a three–gluon vertex), or a $q\bar{q}$ pair. This phase, described by perturbative QCD,

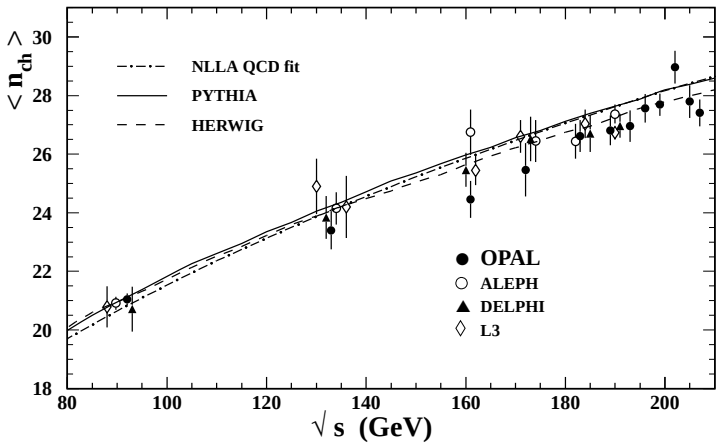


Figure 7: Average charged hadron multiplicity in $e^+e^-$ collisions vs. c.m. energy. The lines represent different predictions of the energy evolution of $\langle n_{ch} \rangle$.

occurs of distances $\sim 10^{-15}$ cm.
iii) In the third phase the quarks and gluons fragment (hadronize) into colourless hadrons (this occurs over distances of $\sim 1$ fm). This phase cannot be analysed with perturbative methods; it is treated with models.
iv) In the 4th phase the produced hadron resonances decay via strong interaction (SI) into "stable" hadrons (e.g. $\rho^0 \to \pi^+\pi^-$); other hadrons decay via the EM interaction ($\Sigma^0 \to \Lambda^0\gamma$, $\pi^0 \to \gamma\gamma$); b-hadrons decay via the weak interaction (with lifetimes of about $10^{-12}$ s). This phase is described by models which include experimental information on lifetimes and branching ratios.

Fig. 7 shows the average charged hadron multiplicity, $\langle n_{ch} \rangle$, in $e^+e^-$ collisions plotted vs $\sqrt{s}$. At the $Z^0$ peak $\langle n_{ch} \rangle = 21.07 \pm 0.11$ [14], at 206 GeV $\langle n_{ch} \rangle \cong 27.7$ [15].

A number of shape parameters (Sphericity, Thrust,...) have been introduced to characterize the global event structure of multihadronic final states. Their studies provide checks of QCD and allow optimization of the Monte Carlos, which play major roles for corrections and for analyses.

For each charged track $k$ of a multihadronic event, one defines the rapidity, the transverse and longitudinal momenta and the variable $x_k = p_k/E_{\rm beam}$.

**$\alpha_s$, the coupling constant of the SI** is a fundamental parameter which may be determined from many types of measurements: (i) from the ratio of 3-jet to 2-jet events, (ii) from shape variables, (iii) from $\Gamma_{\rm h}/\Gamma_\ell = R_Z^0(1+\delta_{\rm QCD})$ , and others. LEP experiments established the flavour independence of $\alpha_s$ and the decrease of $\alpha_s$ with increasing energy [16],[17], Fig. 8. $\alpha_s(\mu)$ can be written as a function of $\ln(\mu^2/\Lambda^2)$, where $\Lambda$ is the QCD scale parameter and $\mu$ is the renormalization

scale

$$\alpha_s(\mu) = \frac{12\pi}{(33-2n_f)\ \ln(\mu^2/\Lambda^2)}\left[1 - \frac{6(153-19n_f)}{(33-2n_f)^2}\ \frac{\ln\ [\ln\ (\mu^2/\Lambda^2)]}{\ln\ (\mu^2/\Lambda^2)}\right] + ... \qquad (13)$$

$n_f$ is the number of active quarks with mass smaller than the energy scale $\mu$. Eq. 13 predicts $\alpha_s \to 0$ as $\mu \to \infty$ (asymptotic freedom). With increasing energy, $n_f$ changes by discrete amounts as a new flavour threshold is crossed. Also $\Lambda$ changes through a flavour threshold, $\Lambda \to \Lambda(n_f)$. $\mu^2$ is usually chosen to be the c.m. energy ($\mu^2 = E_{\rm cm}^2$); a definition $\mu^2 = f \cdot E_{\rm cm}^2$ , with $0.001 < f < 0.01$, gives a better description of the jet production rates.

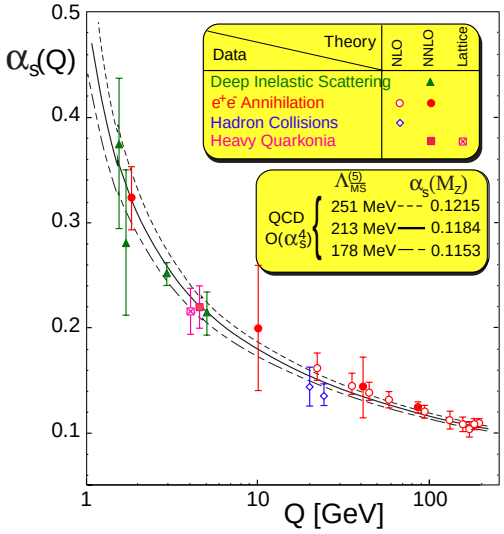


Figure 8: $\alpha_s$ vs $Q = \sqrt{s}$ . The labels NLO and NNLO refer to the order of calculations used. NLO corresponds to $O(\alpha_s^2)$, and NNLO to $O(\alpha_s^3)$. The curves are $O(\alpha_s^3)$ QCD predictions.

**Quark and gluon jet differences.** QCD predicts different coupling strengths for the radiation of an additional gluon from either a quark or a gluon. The coupling strengths are governed by the colour factors for gluon emission, which have the values $C_F = 4/3$ and $C_A = 3$ for radiation from a quark and for a gluon, respectively. These are inclusive factors which need corrections to predict real jets. QCD predicts that a gluon is more likely to radiate a gluon than a quark, and that a gluon jet has a higher particle multiplicity, a softer particle spectrum and is broader than a quark jet of equal energy. Many studies were done at LEP to establish the differences between quark jets and gluon jets [18].

### 3.6 The reactions $e^+e^- \to W^+W^-$ and $e^+e^- \to Z^0Z^0$

For $\sqrt{s} > 2m_W$ one can study the $e^+e^- \to W^+W^-$ reaction, perform precision $W$-physics and test the SM triple boson vertex $ZWW$. The most important diagrams for $W$-pair production are the s-channel $\gamma$/Z exchange, and the t-channel neutrino exchange. Fig. 9a shows the energy dependence of the $e^+e^- \to W^+W^-$ cross section [3],[19]: it has the tipical dependence of a reaction just above threshold. The measured values are consistent with the SM predictions. In a specific model there are 3 independent trilinear gauge couplings (anomalous couplings), which could affect both the total production cross section and the shape of the differential cross-section. Since no deviations from SM predictions have been observed, one can place only upper limits for anomalous couplings.

The results of direct measurements of $m_W$ are given in Table 1.

Table 1: Summary of direct $W$ mass measurements.

| | |
|---|---|
| $p\bar{p}$ colliders | $80.454 \pm 0.060$ GeV |
| LEP2 | $80.450 \pm 0.039$ |
| Average | $80.451 \pm 0.033$ |

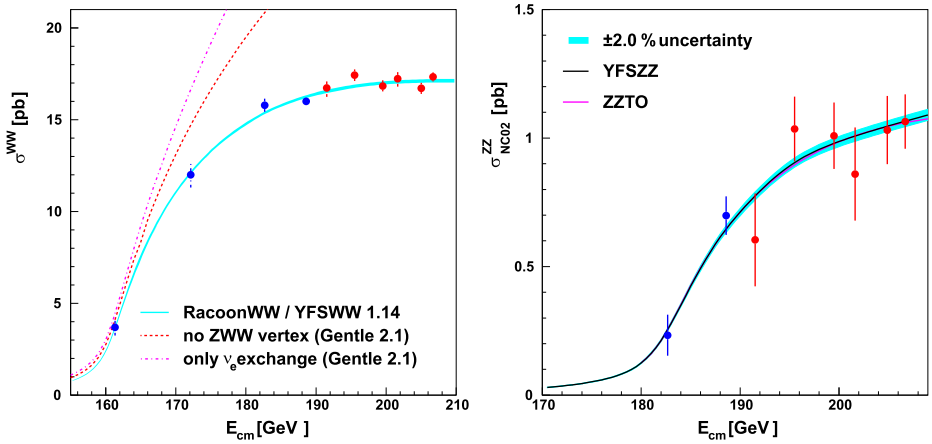


Figure 9: (a) The total $e^+e^- \to W^+W^-$ cross section vs $\sqrt{s}$ compared with the full SM prediction and the predictions without the ZWW vertex and with only the t-channel $\nu_e$ exchange diagram. (b) Cross sections for the reaction $e^+e^- \to Z^0Z^0$ vs $\sqrt{s}$.

Fig. 9b shows the energy dependence of $\sigma(e^+e^- \to Z^0Z^0)$ [19].

## 3.7 New particle searches

The SM has some intrinsic inconsistencies and too many free parameters. It could thus be an effective theory valid in the presently explored energy scale. Very many searches for new physics beyond the SM have been performed, without any positive indication [11],[13],[20],[21]. We shall briefly summarize some searches.

**Searches for SUSY particles.** In supersymmetric (SUSY) models, each normal particle has a supersymmetric partner whose spin differs by half a unit. A new multiplicative quantum number, $R$-parity $= (-1)^{2S+3B-L}$, is introduced, with value +1 for the SM particles and -1 for the SUSY partners. If $R$-parity is conserved, SUSY particles are produced in pairs and they decay to the lightest SUSY particle (LSP), which may be the lowest mass neutralino $\tilde{\chi}_1^0$. In the Minimal Supersymmetric extension of the Standard Model (MSSM) all sparticle masses are determined by 5 parameters: $m_0$ = common mass at the GUT scale, $M_2$ = SU(2) gaugino mass at the EW scale, $\mu$ = mixing parameter of the two Higgs doublets, $A$ = SUSY trilinear coupling. Experimental limits depend on the choise of these parameters.

Higgs bosons. In the MSSM there are 5 scalar Higgs bosons, $h^0$, $H^0$, $A^0$, $H^+$, $H^-$; the neutral ones are searched for with methods similar to those used for the SM Higgs boson; the limits are at the level of those for $H^0_{SM}$.

Charginos. The fermionic SUSY partners of the $W^\pm$ and of the charged Higgs bosons $H^\pm$ mix to form two mass eigenstates for each charge sign, the charginos $\tilde{\chi}^\pm_{1,2}$. They could be pair produced through $\gamma$ or $Z^0$ exchange in the $s$-channel, or through sneutrino exchange in the $t$-channel. The decays yield a neutralino, $\tilde{\chi}^\pm \rightarrow \tilde{\chi}_1^0 +$ .... The experimental signature for pair production and decay is: (i) two acoplanar leptons, (ii) one lepton and one jet, (iii) multi–jets with missing energy/momentum (carried by neutralinos). The existing limits are essentially at the kinematical limit, $m_{\tilde{\chi}^\pm} > 103.5$ GeV [20].

Charged sleptons. Each SM lepton has two scalar partners, the right and left–held sleptons, $\tilde{l}_R$ and $\tilde{l}_L$. They could be pair produced through $s$-channel $\gamma$ or $Z^0$ exchange or through $t$-channel neutralino exchange. The main charged slepton decay is $\tilde{l}^\pm \rightarrow \tilde{l}^\pm + \tilde{\chi}_1^0$. Mass limits are: $m_{\tilde{e}} >$ 99.4 GeV, $m_{\tilde{\mu}} > 96.4$ GeV, $m_{\tilde{\tau}} > 87.1$ GeV [20].

Scalar quarks. A scalar quark, in case of no mixing, could be the lightest charged SUSY particle. The dominant decay mode would be $\tilde{t} \rightarrow c + \tilde{\chi}_1^0$. The event topology would be two acoplanar jets with missing energy/momentum. The limits, assuming a large $\theta_{\rm mix}$, are $m_{\tilde{t}} > 95$ GeV.

Neutralinos. The $\tilde{\gamma}$, $\tilde{Z}^0$, $\tilde{h}^0$,$\tilde{H}^0$ mix to form 4 mass eigenstates, the neutralinos, $\tilde{\chi}_i^0$, i=1,2,3,4. The neutralinos could be pair produced through $s$-channel $Z^0$ exchange or $t$-channel scalar electron exchange. Since the lowest mass $\tilde{\chi}_1^0$ is experimentally unobservable at LEP, the only way to look for $\tilde{\chi}_1^0\tilde{\chi}_1^0$ production is via the reaction $e^+e^- \rightarrow \tilde{\chi}_1^0\tilde{\chi}_1^0\gamma$ or via $\tilde{\chi}_2^0\tilde{\chi}_1^0$ pair production with $\tilde{\chi}_2^0 \rightarrow \tilde{\chi}_1^0 l^+l^-$. The limits obtained are at the level of $m_{\tilde{\chi}_1^0} > 40$ GeV. Higher mass limits are valid only for specific values of the SUSY parameters.

R-Parity violation. If $R$-parity is violated, sparticles could be produced either in pairs or singly and there are no constraints on the nature and on the stability of the LSP. If the LSP decays promptly, the event final states would be characterized by a large fermion multiplicity. If the LSP has a sizeable lifetime one would be able to directly observe sparticles crossing the detector. Both

types of searches have been performed and no positive indication was reported [21]. Limits are quoted in the context of specific models.

**Heavy charged and neutral leptons.** The interest in the search for heavy neutral leptons has increased in view of the possibility that neutrinos have non–zero masses [29]. The typical event topology for pair production and decay ($e^+e^- \to N_l\bar{N}_l \to lW\bar{l}W$) of unstable heavy neutral leptons would be two isolated leptons and two jets of hadrons. Searches for long–lived charged heavy leptons, $e^+e^- \to L^+L^-$, involve topologies with back–to–back charged tracks. For these searches one uses the central tracking detectors and $dE/dx$ measurements. The searches for long–lived neutral leptons assume $e^+e^- \to L^+L^-$, $L^\pm \to L^0W^\pm$. The signature is a pair of acoplanar particles and missing transverse momentum. Present limits extend to masses of about 100 GeV.

**Excited fermions. Compositness.** Composite models predict the existence of excited fermions, $F^*$. They are assumed to have the same electroweak SU(2) and U(1) gauge couplings to the vector bosons ($g$, $g\prime$) as the SM fermions; but they are expected to group into left and right–handed weak isodoublets. Excited fermions could be produced in pairs, $e^+e^- \to F^{+*}F^{-*}$ or singly $e^+e^- \to F^+F^{-*}$. For photonic decays, $F^* \to f\gamma$, the final states involve two leptons and two photons. For the $\bar{\nu}^*\nu^*$ case, the final state involves $2\gamma$ plus missing energy/momentum. The present mass limits for singly produced excited fermions extend to $\sim 202$ GeV.

**Leptoquarks.** Leptoquarks (LQs) are predicted in models which try to explain formally the symmetry between quarks and leptons; they could be produced in pairs and each decays into lepton + quark. At LEP present mass limits are at the level of $> 100$ GeV.

In conclusion: no evidence has been found for particles beyond the SM. The searches will continue at all high energy colliders.

# 4 Lepton–nucleon collisions

The HERA Collider at DESY in Hamburg is an asymmetric $ep$ collider, $E_e \cong 30$ GeV, $E_p \cong 820$ GeV, $E_{cm} \cong 300$ GeV. Two general purpose detectors, $H_1$ and ZEUS, are taking data at luminosities $\mathcal{L} \sim 10^{31}$ cm$^{-2}$ s$^{-1}$ [22]. One of the main physics purposes of these experiments is the study of DIS, either via $\gamma$, $Z^0$ exchange ($ep \to eX$) or via $W^\pm$, $ep \to \nu_e X$.

In the quark–parton model the "current particle" ($\gamma$, $Z^0$, $W^\pm$) emitted by the incoming electron interacts with one of the quarks of the proton. The scattered quark gives rise to a jet of hadrons (current jet). The proton remnants give rise to a second jet (target jet). The process may be described in terms of the four momentum transferred squared $Q^2$ and the energy transferred $\nu = E_e - E_{e\prime}$ (or the variable $x = Q^2/2m_p\nu$ = fraction of the proton momentum carried by the struck quark, and $y = Q^2/xs$).

The cross–section for NC deep inelastic $ep$ scattering may be computed from the elastic electron–quark cross–section. In the quark–parton model the only unknown is the probability $q(x)$ for finding a quark $q$ in the proton carrying a fraction $x$ of the proton momentum. The structure function $F_2^p$ is $F_2^p = \Sigma\, e_q^2\, q(x)$. $F_2$ should be independent of $Q^2$ (Bjorken scaling). For NC deep inelastic scattering the differential cross–sections depend on $F_2(x, Q^2)$.

Because of the large c.m. energy, HERA allows to study the structure function $F_2(x, Q^2)$ at

very small values of x and at very large $Q^2$ [22]. Fig. 10 shows a recent compilation of $F_2$ plotted versus $Q^2$ for different values of $x$. The variation of $F_2$ with $Q^2$ (scale breaking) is predicted by QCD from gluon bremsstrahlung and quark pair creation by gluons. The data are in agreement with this picture. $F_2$ increase considerably at small values of $x$ for any value of $Q^2$. The data indicate that one half of the proton momentum is carried by gluons, which dominate for $x < 0.2$. Even if gluons contribute 50% of the proton momentum, it is difficult to extract the gluon density function $g(x, Q^2)$ because gluons do not contribute directly to DIS in the quark–parton model. One can extract the gluon structure function from the slope of $dF_2/d\ln Q^2$, obtaining $g(x) \sim x^{-(1+\lambda)}$ with $\lambda \sim 0.5$. Thus the number of partons in the proton increases at low values of $x$ (and also at high $Q^2$ for a fixed x value $< 0.1$). This means that when we look inside the proton with a better resolution we see more partons, and the number of gluons tends towards a large value. HERA

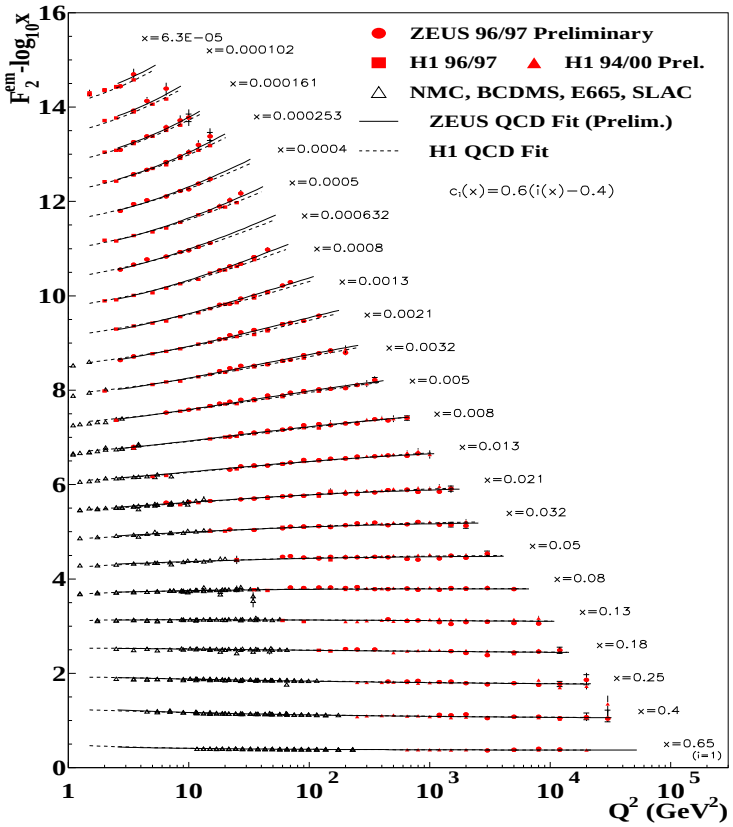


Figure 10: $F_2(x, Q^2)$ at fixed $x$ values as a function of $Q^2$ from different experiments.

allows studies of photoproduction and of diffractive processes. It also allows to search for many new particles; the limits are particularly interesting for leptoquarks: $m_{LQ} > 290$ GeV for first generation scalar leptoquarks [23].

# 5 Hadron–hadron collisions

Most of the recent experimental results on high energy hadron–hadron ($hh$) collisions come from fixed target experiments at CERN, Fermilab and Serpukhov. The upgraded Fermilab $p\bar{p}$ collider started recently data taking at $E_{cm} = 2$ TeV with luminosities $\mathcal{L} > 10^{31}$ cm$^{-2}$ s$^{-1}$. Two general purpose upgraded detectors, CDF and D0, are taking data mainly on large $p_t$ physics.

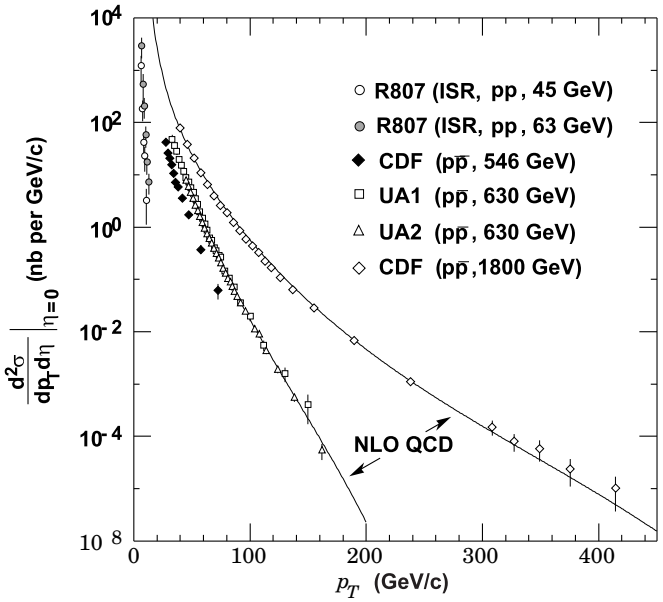


Figure 11: Differential inclusive jet cross–sections at $\eta = 0$ in $hh$ collisions at different c.m. energies.

**Elastic and total cross–sections. Low $p_t$ physics.** The total $p\bar{p}$ cross–section may be written as: $\sigma_{tot} = \sigma_{el} + \sigma_{inel} = \sigma_{el} + \sigma_{sd} + \bar{\sigma}_{sd} + \sigma_{dd} + \sigma_{nd}$, where $\sigma_{el}$ is the elastic cross–section, $\sigma_{sd}$ is the single diffractive cross–section when the incoming proton fragments into a number of particles, $\bar{\sigma}_{sd}$ is the single diffractive cross–section for the fragmentation of the antiproton (at high energies $\sigma_{sd} = \bar{\sigma}_{sd}$), $\sigma_{dd}$ is the double diffractive cross–section, $\sigma_{nd}$ is the non–diffractive part of the inelastic cross–section. The elastic, single diffractive and double diffractive processes give rise to low multiplicity events with particles emitted in the very forward and very backward regions in

the c.m. system. The non–diffractive cross–section is the main part of the inelastic cross–section; non–diffractive processes give rise to high multiplicity events and to particles emitted at all angles. Most of the non–diffractive cross–section concerns particles emitted with low transverse momentum (*low $p_t$ physics*) with properties which change slowly with c.m. energy (*lns physics*).

The total cross–sections for $p\bar{p}$, $pp$, $\pi^- p$, $\pi^+ p$, $K^- p$, $K^+ p$ collisions for c.m. energies between 3 and 70 GeV indicate that as the energy increases, the cross–sections decrease, reach a minimum and then increase. The $K^+ p$ cross–section increases in this entire energy range: its rise was already evident and established at Serpukhov energies. All the differences $\sigma_{tot}(\bar{x}p) - \sigma_{tot}(xp)$ decrease with increasing energy[24]. The slope parameter $b$ for $p\bar{p}$ elastic scattering keeps increasing up to $\sqrt{s} = 1.8$ TeV, at a rate which is probably larger than $\ln s$. The total elastic $p\bar{p}$ cross–section continues to rise at a rate close to $\ln^2 s$ or larger. Therefore the ratio $\sigma_{el}/\sigma_{tot}$ increases with energy, reaching the value of about 0.24 at $\sqrt{s} = 1.8$ TeV. This value is still below the black disk value of 0.5, though the center of the proton has become more opaque, almost black. Present values of $\rho$, the ratio of the real to the imaginary part of the $p\bar{p}$ elastic scattering amplitude, obtained from elastic scattering data in the Coulomb–Nuclear interference region, follow the dispersion relation predictions.

The average charged particle multiplicity has increased with energy reaching a value $< n_{ch} > \cong$ 40 at $E_{cm} \cong 1.8$ TeV.

In most elastic scattering analyses the polarization effects are neglected: such effects are thought to decrease as the energy increases and they are small in the forward direction. But sizable and measurable spin and asymmetry effects were observed at $p_{lab} = 28$ GeV/c and at high $p_t$, where the cross section for $pp$ elastic scattering with spins parallel is about four times larger than the cross section for spins antiparallel ($p_t \sim 2 - 3$ GeV/c). Spin effects need to be investigated more systematically, both experimentally and theoretically.

**Large $p_t$ physics.** A relatively small part of the non–diffractive cross–section is due to central collisions among the colliding particles and gives rise to high $p_t$ jets of particles emitted at large angles (*large $p_t$ physics*). The contribution of jet physics increases with c.m. energy. The two–jet production in $p\bar{p}$ collisions, $p+\bar{p} \to 2$ jets $+X$, is due to parton–parton processes [25]. Fig. 11 shows a compilation of inclusive jet cross–sections measured in hadron–hadron collisions at different c.m. energies. Good agreement is found with the QCD prediction, thus excluding new physics, such as that expected from subconstituent contact interactions [26].

**The top quark.** The CDF and D0 collaborations found the top quark and are studying the detail of its production and decay [27]. In $p\bar{p}$ collisions the dominant channels are via quark–antiquark annihilation or gluon–gluon fusion: $q + \bar{q} \to t + \bar{t}, \quad g + g \to t + \bar{t}$. The dominant decays of the top quark are

$$t \to W^+ + b, \quad t \to W^+ + (s \text{ or } d), \quad t \to g + W^+ + (b, s \text{ or } d)$$

and likewise for $\bar{t}$. The present $t$ mass value is quoted in Fig. 4.

**New particle searches.** The CDF and D0 experiments give 95% CL limits on many new particles, in particular: $m_{LQ} > 160(148)$ GeV for second (third) generation scalar LQs, $m_{Z'} > 670$ GeV, $m_{W'} > 755$ GeV [28].

# 6 Conclusions

Experiments at the large colliders (LEP, SLC, Fermilab, HERA) and at lower energies collected an impressive amount of data, which together with new theoretical calculations, provide stringent tests of the Standard Model.

The main physics results may be summarized as follows: three neutrino families, lepton universality, precise determination of electroweak and strong parameters ($m_Z$, $\Gamma_Z$, $\sin^2\theta_W$, $m_W$, $m_t$, $\alpha_s$, .....), the flavour independence of $\alpha_s$, the running of the strong and of the E.M. coupling costants, the existence of the triple boson vertex $Z^0W^+W^-$, the determination below threshold of the mass of the top quark and of its discovery above threshold, possible indications and limits on the $H^0_{SM}$ mass, $b$ and $\tau$ physics, precise measurements of the lifetimes of short lived particles, studies of QCD at large and small $p_t$, detailed studies of multihadron final states and of the difference between quark and gluon jets, the deeper structure of the proton and of the photon, etc. All experiments gave increasingly better limits on new particles and new phenomena. Let us hope that the new increases in energy and luminosity will really open up a new field. These results have also strong implications in the astroparticle physics field [29].

Experiments at lower energies provided information on direct CP violation in the $K^0\bar{K}^0$ system and of CP violation in $B^0\bar{B}^0$, have shown the importance of understanding the spin of the proton (spin crisis) and of polarization measurements, the first indications for the quark–gluon plasma, etc.

One should not neglect the very large number of Diploma, Laurea and PhD theses using high energy data and the strong impact of fundamental high energy physics on the public understanding of science.

We would like to thank the members of the OPAL Collaboration for their cooperation; we acknowledge the collaboration of D. Bonacorsi, F. Fabbri, P. Giacomelli, S. Marcellini, and other members of the Bologna groups.

# References

[1] G.Giacomelli and R.Giacomelli, *Results from high–energy $e^+e^-$ collisions*, Proc. of the $5^{th}$ School on Non Accelerator Particle Astrophysics, Edizioni Universitá di Trieste (1999).

[2] LEP Coll. and the Electroweak working group, SLD heavy flavour and electroweak groups, *A combination of preliminary LEP electroweak measurements*, CERN-EP/2001-021 (2001).
OPAL Coll., G.Abbiendi et al., *Eur. Phys. J.* C **19**, 587 (2001).

[3] D.Charlton, *Experimental tests of the Standard Model*, BHAM-HEP-01-02, Proc. of Int. Conf. EPS–HEP, Budapest (2001).
W.Venus, *A LEP summary*, Proc. of Int. Conf. EPS–HEP, Budapest (2001).
S.Mele, *Combined fit to the Electroweak data and constraints on the Standard Model*, http://l3www.cern.ch/conferences/talks2001.html.
Numbers and plots in http://lepewwg.web.cern.ch/LEPEWWG/

[4] NA48 Coll., V.Fanti et al., *Phys. Lett.* B **465**, 335 (1999); A.Lai et al., *A precise measurement of the direct CP violation parameter* $Re(\varepsilon'/\varepsilon)$, CERN-EP/2001-067, Eur. Phys. J., to be published.
KTeV Coll., A.Alavi-Harati et al., *Phys. Rev. Lett.* **83**, no. 1, 22 (1999).

[5] BABAR Coll., B.Aubert et al., *Phys. Rev. Lett.* **87**, 091801 (2001).
BELLE Coll., K.Abe et al., *Phys. Rev. Lett.* **87**, 091802 (2001).

[6] SMC Coll., B.Adeva et al., *Phys. Rev.* D **58**, 112001 (1998).
A.Feltham., *Prog. Part. Nucl. Phys.* **36**, (1996).

[7] OPAL Coll., K.Ackerstaff et al., *Standard Model measurements in* $e^+e^-$ *collisions at* $\sqrt{s} = 189$, OPAL Physics Note PN368 (1998).

[8] BES Coll., J.Z.Bai et al., hep-ex/0102003 (2001).

[9] H.Burkhardt and B.Pietrzyk, *Phys. Lett.* B **513**, 46 (2001).

[10] A.D.Martin et al., *Phys. Lett.* B **492**, 69 (2000).

[11] G.Giacomelli and P.Giacomelli, *Nuovo Cimento Riv.* **16**, vol. 3, 1 (1993).

[12] LEP Coll., LEP working group for Higgs boson searches, *Search for the Standard Model Higgs*, CERN-EP/2001-055 (2001).

[13] P.Igo-Kemenes, *Searches for Higgs bosons in the SM and in the MSSM at LEP*, Proc. of 7th topical seminar on the legacy of LEP and SLC, Siena (2001)

[14] D.E. Gromm et al., *Eur. Phys. J.* C **15**, 1 (2000).

[15] ALEPH Coll., *QCD measurements in* $e^+e^-$ *annihilations at 206 GeV*, Conference Note, ALEPH 2001-007 (2001);
L3 Coll., *Study of hadronic event structure and* $\alpha_s$ *determination at* $192 < \sqrt{s} < 208$ *GeV*, L3 note 2670 (2001);
OPAL Coll., *Measurements of SM processes in* $e^+e^-$ *collisions at* $\sqrt{s} \sim 203 - 209$ *GeV*, OPAL Phys. Note PN469 (2001).

[16] S.Bethke, *J. Phys.* G **26**: R27 (2000).

[17] G.Dissertori, hep–ex/0105070, Proc. of the 13th meeting on Physics at LEP, Rome (2001).

[18] OPAL Coll., G.Abbiendi et al., CERN-EP/2001-076 (2001), submitted to Eur. Phys. J. C, hep–ex/0111013.

[19] LEP Coll. and LEP WW working group, *LEP W–pair, Z–pair and single W cross section results for the Summer 2001 Conferences*, LEPEWWG/XSEC/2001-03 (2001). Numbers and plots in http://lepewwg.web.cern.ch/LEPEWWG/lepww/4f/

[20] B.Clerbaux, *Search for MSUSY particles at LEP*, Proc. of Int. Conf. EPS–HEP, Budapest (2001).
WEB page: http//lepsusy.web.cern.ch/lepsusy/.

[21] S. Braibant, *Other searches at LEP*, OPAL Conf. Report CR-469, Proceedings 36th Rencontres de Moriond (2001).
M.C.Espirito Santo, *Search for SUSY with R-parity Violation at LEP*, Proc. of Int. Conf. EPS–HEP, Budapest (2001).

[22] B.Stella, *Proton structure functions at HERA*, invited paper at International Symposium on Hadrons and Nuclei, Seoul, 2001.
H1 Coll., C.Adloff et al., *Eur. Phys. J.* C **21**, 33 (2001).
ZEUS Coll., J. Breitweg et al., *Phys. Lett.* B **487**, 1,53 (2000).

[23] X.Liu, *Search for Leptoquarks and contact interactions at HERA*, Proc. of Int. Conf. EPS–HEP, Budapest (2001).

[24] G.Giacomelli, hep-ex/0006038 (2000).
A.Carroll et al., *Phys. Rev. Lett.* **33**, 928 (1974).
S.P.Denisov et al., *Phys. Lett.* B **36**, 415 (1971).

[25] SFM Coll., A.Breakstone et al., *Z. Phys. J.* C **23**, 1 (2001).

[26] CDF Coll.,T.Affolder et al., *Phys. Rev.* D **64**, 032002 (2001).
D0 Coll., B.Abbot et al., *Phys. Rev.* D **64**, 032003 (2001).

[27] CDF Coll., T.Affolder et al., *Phys. Rev. Lett.* **87**, 102001 (2001).
D0 Coll., B.Abbot et al., *Phys. Rev. Lett.* **83**, 4769 (1999).

[28] E.Nagy, *Search for R-parity violation and exotica at Tevatron*, Proc. of Int. Conf. EPS–HEP, Budapest (2001).

[29] G.Giacomelli et al., hep-ex/0110021 (2001);
D.Bakari et al., hep-ex/0004019 (2000);
G.Giacomelli and L.Patrizii, hep-ex/0112009 (2001);
Proc. of the $6^{\text{th}}$ School on Non Accelerator Astroparticle Physics, World Scientific (2001): S.Bottino, *Dark matter*; A.De Rujula, *Beyond the Standard Model*.